Fluorescence Dynamics of Dye Probes in Micelles

Nakul C. Maiti, M. M. G. Krishna, P. J. Britto, and N. Periasamy*

Chemical Physics Group, Tata Institute of Fundamental Research, Homi Bhabha Road, Bombay 400 005, India

Received: July 16, 1997; In Final Form: September 30, 1997[⊗]

The fluorescence depolarization dynamics of organic fluorescent dye probes (nile red, cresyl violet, DODCI, rhodamine B, and rhodamine DPPE) were studied in cationic, anionic, and neutral micelles by picosecond time-resolved single-photon-counting technique. The fluorescence anisotropy decay of the dye intercalated inside the micelle is a two-exponential function. The anisotropy decay was interpreted by using a model of rotational (wobbling) and translational diffusion of the dye in the micelle coupled with the rotational motion of the micelle as a whole. The rotational and translational diffusion coefficients of the dye, the order parameter, and the semicone angle for the wobbling diffusion in the micelle were determined. The concept of "microviscosity" in the micelle was critically discussed in the light of the rotational and translational diffusion coefficients and their temperature dependence.

Introduction

The depolarization of fluorescence of organic dye molecules in liquids is one of the powerful techniques for the investigation of the tumbling or rotational motion of the molecule on the picosecond to nanosecond time scale.[1] The fluorescence anisotropy decay for a number of organic dye molecules was found to be single exponential in pure solvents,[2−11] and the rotational dynamics of the molecule resembles that of an ellipsoid or a sphere. There are also a few reports where the anisotropy decay in liquids was found to be biexponential.[12−15] In general, the rotational diffusion coefficient is inversely related to the viscosity of the solvent by the Stokes−Einstein equation for neutral molecules or the Debye−Stokes−Einstein equation for charged molecules. In microheterogeneous media such as micelles and membranes the rotational dynamics of the dye is fundamentally different from that in homogeneous media in two aspects. First, the existence of an aqueous/nonaqueous interface leads to an orientationally nonrandom equilibrium distribution of the molecules, and second, the molecular dynamics is highly restricted. Understanding the fluorescence dynamics in microheterogeneous media such as micelles is helpful for the interpretation of time-resolved fluorescence dynamics in complex but important biological systems.

An organic molecule is readily soluble in an aqueous micellar solution because of the favorable (hydrophobic) sites for solubilization in the micellar aggregate.[16−18] It is well established that the site of solubilization is near the interface for a wide variety of organic molecules.[19−21] The fluorescence anisotropy decay of the organic molecule is directly related to the reorientation dynamics of the excited molecules and hence best suited for the investigation of local molecular dynamics near the site. A unique feature of the nanometer size micelle is the fluorescence depolarization as a result of reorientation due to translational motion of the molecule along the surface. In homogeneous media and in planar membranes the translational motion of the molecule does not reorient the molecule. Previous studies have considered various models for the reorientation dynamics of the molecule inside the micelle.[22−26] All these studies, except that of Quetevis et al.,[26] ignore the contribution of translational motion to the anisotropy decay. The fluorescence anisotropy decay of a fluorescent molecule in a spherical micelle is best described by a model of restricted rotational motion of dye (wobbling-in-cone model) coupled with translational motion on the surface and rotation of the whole micelle. This model is used in the present study of fluorescence anisotropy decay of five organic dye probes in cationic, anionic, and neutral micelles.

The fluidity of organized molecular assemblies such as micelles and membranes are frequently estimated by the quantitative parameter called microviscosity.[16,17,27,28] The concepts involved in the estimation of microviscosity in micelles are the same as those for the estimation of viscosity in pure liquids, namely, applicability of Stokes−Einstein equations for the translational and rotational diffusion coefficients. The concept of microviscosity has been critically discussed in the light of the diffusion coefficients for the organic probes in micelles.

Experimental Section

Materials. Laser grade dyes, nile red, cresyl violet perchlorate (CV), 3,3′-diethyloxadicarbocyanine iodide ((DODCI), and rhodamine B, were used as received from Exciton, Inc. Rhodamine labeled with a lipid, rhodamine-DPPE, was purchased from Molecular Probes. Figure 1 shows the chemical structures of the five dyes. The fluorescence decays of these dyes in methanol were single exponential, indicating the purity of the dye. Sodium dodecyl sulfate (SDS) (Sigma Chemical Co.), cetyltrimethylammonium bromide (CTAB) (Aldrich Chemicals), and Triton-X 100 (TX) Sigma Chemicals) were checked to be fluorescence-free and used as received. Micellar samples were prepared by stirring the dye in warm solutions of surfactant in deionized water for about 1 h.

Fluorescence decays were measured using a pirosecond laser coupled with a time-correlated single-photon-counting (TCSPC) spectrometer described previously.[29,30] The fluorescence decays were obtained for three orientations of the emission polarizer: magic angle of 54.7° and parallel and perpendicular orientations with respect to the excitation polarization. Typically, the peak count in the fluorescence decays was $(1-2) \times 10^4$ for lifetime measurements and $(2-3) \times 10^4$ for anisotropy decays. The perpendicular component of the fluorescence decay was corrected for the *G*-factor of the spectrometer, which was determined[31] as follows. The *G*-factor (defined as the ratio of the sensitivities of the spectrometer for parallel and perpendicular

* Author for correspondence. Fax: 091 22 215 2110/2181. email: peri@tifrvax.tifr.res.in.

⊗ Abstract published in *Advance ACS Abstracts,* November 15, 1997.

S1089-5647(97)02312-2 CCC: $14.00

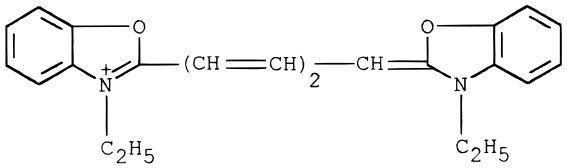

DODCI

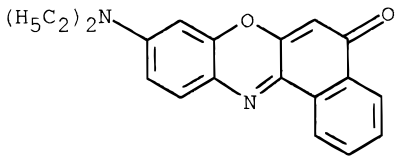

Nilered

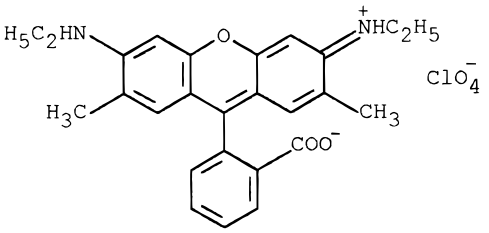

Rhodamine B

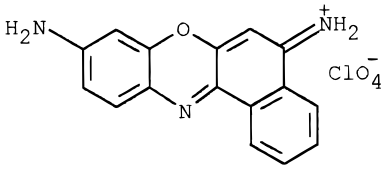

Cresyl Violet

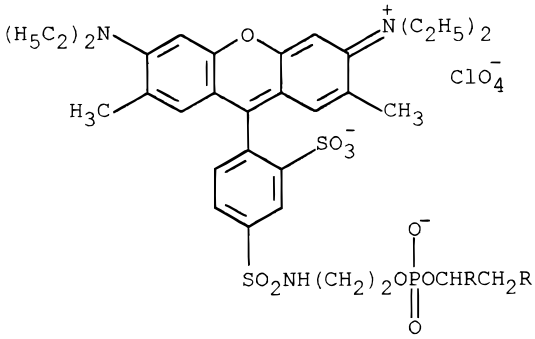

R = −OCO(CH2)14CH3

Rhodamine DPPE

Figure 1. Molecular structure of dyes.

polarization of light) was determined using cresyl violet in methanol ($\tau_f = 3.23$ ns, $\tau_r = 130$ ps) for which the fluorescence emission is practically depolarized at times greater than 1 ns after excitation. The *G*-factor is the ratio of the collection times for which the tails of the fluorescence decays of parallel and perpendicular components match exactly. Steady-state anisotropy measurements were done using a Shimadzu RF-540 spectrofluorimeter.

Fluorescence Decay Data Analysis. The fluorescence decays were fitted to the appropriate mathematical functions by the standard iterative method of convolution with instrument response function and comparison with raw data until the good fit criteria (lowest value for reduced χ^2 and random distribution of weighted residuals) were attained.[32] The parameter values were adjusted in successive iterations based on the Levenberg−Marquardt method.[33,34]

The fluorescence decay at magic angle polarization was fitted to a single exponential to get the lifetime. In a few cases (CV and DODCI in CTAB and TX and rhodamine B) the fluorescence decay is biexponential. In these cases, the intensity decay function $I(t)$ is given by eq 1,

$$I(t) = \alpha I_1(t) + (1 - \alpha) I_2(t) \tag{1}$$

where $I_1(t)$ and $I_2(t)$ are the single-exponential decays with lifetimes τ_{f1} and τ_{f2} in the two phases (water and micelle) (CV and rhodamine B) or two forms of the dye in the micelle (DODCI) and α is the fractional intensity associated with τ_{f1}.

Parallel and perpendicular components of fluorescence decays were fitted simultaneously[35,36] to eqs 2 and 3 in all cases except those cases where the dye is distributed in two phases.

$$I_{||}(t) = (1/3) I(t)[1 + 2r(t)] \tag{2}$$

$$I_{\perp}(t) = (1/3) I(t)[1 - r(t)] \tag{3}$$

where $r(t)$ is the anisotropy decay. The basic approach to the fitting strategy has been discussed in detail before.[7] An additional criterion used in the present work is to seek agreement between the values of steady-state anisotropy measured in an independent experiment and the value calculated from the anisotropy decay parameters using eq 5, 7, or 10. In pure solvents (water and *n*-butanol) $I(t)$ is a single exponential and $r(t)$ is also a single exponential (eq 4):

$$r(t) = r_0 \exp(-t/\tau_r) \tag{4}$$

where r_0 is the initial anisotropy and τ_r is the reorientation time. The fitting of eqs 2 and 3 to the decay data requires optimization of seven parameters (two scale factors, τ_f, τ_r, r_0, and two shift parameters). The steady-state anisotropy is calculated using eq 5.

$$r_{ss} = r_0\tau_r/(\tau_f + \tau_r) \quad (5)$$

In cases where the dye is present only in the micelle, $I(t)$ is a single exponential and $r(t)$ is biexponential (eq 6).

$$r(t) = r_0[\beta \exp(-t/\tau_{slow}) + (1-\beta)\exp(-t/\tau_{fast})] \quad (6)$$

Data analysis using eqs 2 and 3 and eq 6 for $r(t)$ requires optimization of nine parameters (τ_f, r_0, τ_{slow}, τ_{fast}, β, two scale factors, and two shift parameters). Of these τ_f is known from the analysis of decay at magic angle polarization, and this value was fixed in the analysis. Fixing τ_f helps to recover reproducible values for the anisotropy decay parameters. r_{ss} is calculated using eq 7.

$$r_{ss} = r_0[\beta\tau_{slow}/(\tau_f + \tau_{slow}) + (1-\beta)\tau_{fast}/(\tau_f + \tau_{fast})] \quad (7)$$

In the case of CV in CTAB or TX and rhodamine B, the dye is distributed in two phases. Equations 8 and 9 are used to fit the polarized fluorescence decays.

$$I_{||}(t) = \alpha(1/3)I_1(t)[1 + 2r_1(t)] + (1-\alpha)(1/3)I_2(t)[1 + 2r_2(t)] \quad (8)$$

$$I_{\perp}(t) = \alpha(1/3)I_1(t)[1 - r_1(t)] + (1-\alpha)(1/3)I_2(t)[1 + r_2(t)] \quad (9)$$

α is the fractional intensity in water, $I_1(t)$ and $I_2(t)$ are the intensity decays, and $r_1(t)$ and $r_2(t)$ are the anisotropy decays in water and micelle. In these cases the fluorescence decay (at magic angle polarization) is biexponential (eq 1), and thus, $I_1(t)$, $I_2(t)$, and α in eqs 8 and 9 are known. Further, the anisotropy decay function of $r_1(t)$ for the aqueous phase can be determined independently. Fixing all these parameters (α, τ_{f1}, τ_{f2}, r_0, and τ_{r1}) with known values reduces the number of parameters to be optimized to those of $r_2(t)$, which describes the anisotropy decay in the micellar phase. It was found that a biexponential function, eq 6, gave a satisfactory fit. In these cases r_{ss} is calculated by eq 10.

$$r_{ss} = \frac{r_0\left[\alpha\tau_{f1}\frac{\tau_{r1}}{\tau_{r1}+\tau_{f1}} + (1-\alpha)\tau_{f2}\left\{\frac{\beta\tau_{slow}}{\tau_{slow}+\tau_{f2}} + (1-\beta)\frac{\tau_{fast}}{\tau_{fast}+\tau_{f2}}\right\}\right]}{\alpha\tau_{f1} + (1-\alpha)\tau_{f2}} \quad (10)$$

Criteria for Good Fit. A good fit of the raw data is indicated by a random distribution of the weighted residuals[32] defined as,

$$r_i = \frac{(F_i^c - F_i^e)}{(F_i^e)^{1/2}} \quad (11)$$

where F_i^e and F_i^c are experimental and calculated intensities. There are several tests to examine the randomness of the weighted residuals. The standard practice is to examine the distribution of residuals in the following order: (1) check visually the plot of residuals vs channel number for randomness, (2) calculate the value of χ^2 (eq 12) and check if the value is in the range 0.8−1.2.

$$\chi^2 \approx \frac{1}{N}\sum_{i=1}^{N} r_i^2 \quad (12)$$

In addition, an autocorrelation plot of residuals and the value of the Durbin−Watson parameter[32] are also used in this work, wherever necessary.

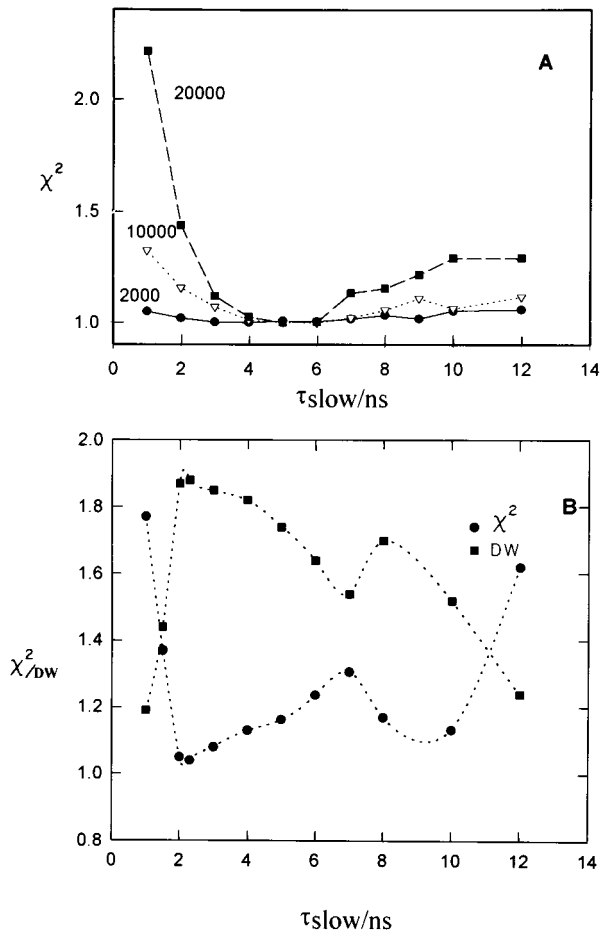

Figure 2. (A) Plot of χ^2 vs τ_{slow} obtained from the analysis of simulated fluorescence decays. See text for details. The peak count in the parallel component of the simulated decay is 2000, 10 000, and 20 000. (B) Plot of χ^2 and DWP (DW) vs τ_{slow} for cresyl violet in SDS micelle. Peak count in the parallel component of fluorescence decay is 25 000.

In the case of simultaneous fit of parallel and perpendicular components of fluorescence decay data the above criteria were adequate for the simple cases where $I(t)$ and $r(t)$ were single-exponential functions as in pure solvents. However, in cases of micellar systems where $I(t)$ or $r(t)$ or both are biexponential the following additional criteria were found to be useful in deciding the goodness of fit: (1) a visually acceptable fit of the raw data of $r(t)$ (see Figure 5) and (2) a good agreement between the value of r_{ss} calculated from the optimized values of anisotropy parameters and r_{ss} measured experimentally by steady-state fluorescence.

The error associated with the value of the optimized parameters depends upon the number of parameters simultaneously optimized. Occasionally, the value of a parameter may not be properly estimated at all. That is, the criteria for goodness of fit can be satisfied for a wide range of values of a less sensitive parameter. An example of this type is the optimization of the value of τ_r using a fluorophore for which $\tau_f \ll \tau_r$. It is necessary therefore to estimate the error in anisotropy decay times, especially for τ_{slow} in micellar systems. This was done using the plot of χ^2 vs τ_{slow}. To obtain these plots τ_{slow} was varied as a fixed parameter in the data analysis. The efficiency of this method was tested with simulated fluorescence decay data (see below).

Fluorescence decay data (parallel and perpendicular components) were simulated (40 ps/ch) using an instrumental response

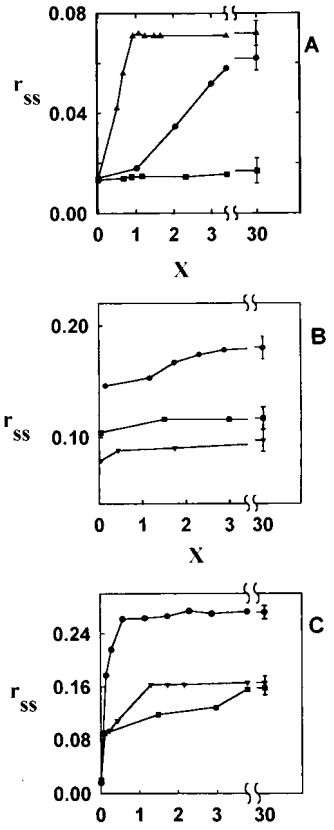

Figure 3. Plot of steady-state anisotropy (r_{ss}) vs X ([surfactant]/cmc). (A) Cresyl violet in different micelles: SDS (▲), TX-100 (●), and CTAB (■). (B) Nile red in different micelles; SDS (▲), TX-100 (●), and CTAB (■) (nile red being insoluble in water, there is no data for $X = 0$). (C) DODCI in different micelles: SDS (▲), TX (●), and CTAB (■).

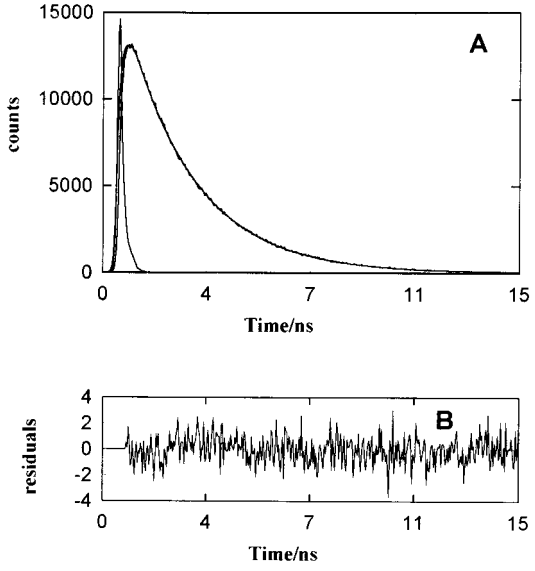

Figure 4. Fluorescence decay profile of 5 μM nile red (5 μM) in SDS (30 mM) recorded at magic angle polarization, $\lambda_{ex} = 580$ nm, $\lambda_{em} = 640$ nm. $\tau_f = 2.43$ ns, $\chi^2 = 1.05$. (A) Instrument response function and the fluorescence decay. The solid line through the fluorescence decay is the best fit for a single-exponential function. (B) Distribution of the weighted residuals for the best fit of fluorescence decay.

function (experimentally determined) for the following values for fluorescence (single exponential) and anisotropy (biexponential) decay parameters: $\tau_f = 2$ ns, $\tau_{fast} = 0.5$ ns, $\tau_{slow} = 5$ ns, $\beta = 0.5$, and $r_0 = 0.3$. The peak counts in the simulated data for the parallel component were 2000, 10 000, and 20 000

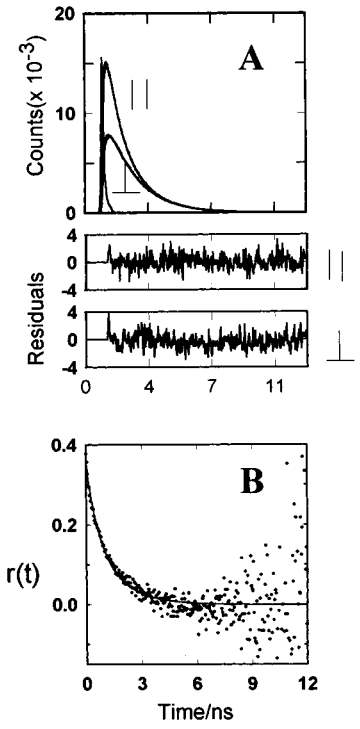

Figure 5. Parallel and perpendicular components of fluorescence decay profiles of DODCI in SDS micelles ([DODCI] = 1 μM, [SDS] = 30 mM, $\lambda_{ex} = 580$ nm, $\lambda_{em} = 610$ nm). The upper curve is $I_{||}$ and the lower curve is $I_{\perp}$ plotted against time (ns). The weighted residual distributions for fits of parallel and perpendicular fluorescence decays are shown below the fluorescence decay curves, $\chi^2 = 1.08$. (B) Fluorescence anisotropy decay profile of DODCI in SDS. Solid line is the calculated curve (see text for details).

before the addition of Poisson noise.[37] Each of these simulated data sets were analyzed to extract best-fit parameters for the anisotropy decay. Figure 2A shows plots of χ^2 vs τ_{slow} obtained in the analysis of simulated fluorescence decay data. It is observed that χ^2 is insensitive to τ_{slow} if the peak count is only 2000. It will be impossible to determine τ_{slow} in this case. When the peak count is 20 000, χ^2 is sufficiently sensitive to τ_{slow} to indicate a good minimum at $\tau_{slow} = 5$ ns, and therefore one can rule out τ_{slow} values outside the range of 5 ± 0.5 ns as unacceptable. It is clear from the analysis of simulated data that a peak count of 2×10^4 or above is desirable in the experimental data in order to obtain an accurate estimate of τ_{slow}. Figure 2B shows the plot of chi-square vs τ_{slow} for a micellar sample (cresyl violet in SDS, with a peak count of 2.5×10^4) for which $I(t)$ is a single exponential ($\tau_f = 2.94$ ns) and $r(t)$ is biexponential ($r_0 = 0.32$, $\tau_{fast} = 0.43$ ns, $\tau_{slow} = 2.05$ ns, and $\beta = 0.35$). χ^2 was minimum at 2 ns, and a reasonable estimate is $\tau_{slow} = 2.0 \pm 0.1$ ns. Interestingly, the plot also shows that χ^2 has another minimum at $\tau_{slow} \approx 9$ ns. However, for this value of τ_{slow} the weighted residuals fail the test of serial correlation, as indicated by the lower value of the Durbin−Watson parameter (Figure 2B), namely, 1.7 compared to 1.9 for $\tau_{slow} = 2$ ns.

Results

Steady-state anisotropy (r_{ss}) is an excellent indicator of the efficiency of solubilization of the dye in the three micelles. The dye molecule bound to the micelle tumbles slowly compared to the free dye in water, and hence r_{ss} increases when the surfactant concentration is increased. r_{ss} attains a maximum value when all the dye molecules are micellized. The plots of r_{ss} vs x (=[surfactant]/cmc, where cmc is the critical micelle concentration) for three dyes (nile red, cresyl violet, and

TABLE 1: Fluorescence Intensity and Anisotropy Decay Parameters for the Fluorescence Dye Probes in Water, Butanol, and Micelles[a]

dye/solvent/micelle	τ_{f1} (ns)	τ_{f2} (ns)	α_1	r_0	τ_{slow} (ns)	τ_{fast} (ns)	β	r_{ss}
nile red								
butanol	3.90		1	0.313	0.43		1	0.031
SDS	2.43		1	0.329	1.99	0.57	0.36	0.090
CTAB	2.94		1	0.339	3.09	0.64	0.51	0.120
TX-100	3.75		1	0.323	7.65	1.80	0.63	0.180
cresyl violet								
water	2.04		1	0.330	0.15		1	0.020
butanol	3.18		1	0.340	0.75		1.0	0.060
SDS	2.94		1	0.322	2.05	0.43	0.35	0.070
CTAB	2.04	1.67	0.64	0.320	3.83	0.99	0.45	0.120
TX-100	2.06	1.23	0.77	0.310	5.39	0.81	0.63	0.180
DODCI								
water	0.64		1	0.318	0.22		1.0	
butanol	1.16		1	0.366	0.40		1.0	0.094
SDS	1.52		1	0.331	2.01	0.55	0.57	0.074
CTAB	1.75	0.46	0.86	0.342	4.08	0.71	0.59	0.160
TX-100	1.81	0.89	0.97	0.328	5.39	0.59	0.77	0.200
rhodamine								
water	1.61		1	0.385	0.18		1	0.040
butanol	3.12		1	0.352	0.54		1	0.032
SDS	2.88	1.5	0.85	0.383	2.33	0.51	0.57	0.205
CTAB	2.10	1.52	0.79	0.358	4.22	1.16	0.31	0.150
TX-100	2.89	1.49	0.77	0.368	7.78	1.60	0.56	0.190
rhod-DPPE								
SDS	3.10		1	0.250	3.62	1.88	0.38	0.100
CTAB	2.07		1	0.342	7.09	0.87	0.71	0.218
TX-100	2.67		1	0.334	21.30	2.50	0.48	0.220

[a] λ_{ex} (nm) and λ_{em} (nm) are as follows: 580 and 640 (nile red, cresyl violet), 580 and 610 (DODCI), 570 and 610 (rhodamine and rhod-DPPE).

DODCI) in the three micelles (SDS, CTAB, and TX) are shown in Figure 3. For $x = 0$, the steady-state anisotropy is that of the dye in water, if the dye is soluble. For $0 < x \leq 1$, a region in which the surfactant concentration is below the cmc, the micelles are not fully formed. However, the steady-state anisotropy increases in this region also because the dye may be associated with incompletely aggregated micellar structures and hence the fluorescence depolarization is less. If the dye has a greater affinity for the micelle, then the increase in the anisotropy will be sharp in the region $0 < x < 1$ and the value becomes constant for $x > 1$. As seen in the plots in Figure 3B, the dye nile red, which is insoluble in water, has a greater affinity for micellization in all three micelles. A similar behavior (Figure 3C) is also observed for the cationic dye DODCI in all three micelles. For these two dyes the solubilization of the dye may be considered complete for $5 < x < 10$, and the fraction of the dye remaining in water is negligible. In the case of cresyl violet the anisotropy plots (Figure 3A) indicate that a constant value is attained for $x > 1$ in SDS, but the plateau value is not attained in CTAB and TX even for $x \approx 30$. It is presumed that the cationic dye CV has a greater affinity for water than the micellar environment of positively charged CTAB or neutral TX. The preferential micellization in SDS is attributable to the Coulombic attraction between the negatively charged SDS and the positively charged dye.

The fluorescence decay of the dyes in micelles and in pure solvents (water and *n*-butanol) were investigated. The dye concentration was below 10 μM in all the cases. The fluorescence decay in water and *n*-butanol were single exponential, and the lifetimes are given in Table 1. For fluorescence decay measurements in the micelles, the surfactant concentration used were well above the cmc: typically, 60 mM (SDS), 28 mM (CTAB), 10 mM (TX). The concentration of micelle ([micelle] = ([surfactant] − cmc)/aggregation number) was 0.07 mM for TX, 0.85 mM for SDS, and 0.44 mM for CTAB. The corresponding x values are 6.8 for SDS, 30.4 for CTAB, and 38.5 for TX (calculated using known values (Table 2) for cmc and aggregation number at 25 °C: 8.8×10^{-3} M and 62 (SDS), 9.2×10^{-4} M and 60 (CTAB), 2.6×10^{-4} M and 143 (TX)). The ratio of the micelle to dye (typically 1−5 μ M) concentration is >100 for all cases in SDS and CTAB and >50 in TX. For this ratio, the dye is distributed as one per micelle (Poisson law). The fluorescence decays were single exponential for all dyes in SDS except rhodamine B. The values of lifetimes and amplitudes are given in Table 1. The observation of a biexponential decay for CV in CTAB and TX and rhodamine B in all micelles is due to the distribution of the dye in aqueous and micellar phases. It was observed that one of the two lifetimes was close to the lifetime (2.04 ns) for CV in water. Figure 4 shows a plot of the fluorescence decay of CV in SDS and the results of fitting the decay data to a single-exponential function.

TABLE 2: Radii and Other Physical Parameters of Different Micelles and τ_m at 25 °C

micelle	charge (surface)	N_{agg}[f]	cmc[f] (mM)	core radius r_c (Å)	hydrodynamic radius, r_h (Å)	τ_M[a] (ns)
SDS	(−)	62	8.0	16.7[b]	20.7[c], 21.0[d]	8.3
CTAB	(+)	60	0.92	21.7[b]	25.7[c]	15.4
TX-100	(neutral)	143	0.26	43[e]	43	72

[a] $\tau_M = 4\pi r_h^3 \eta/(3kT)$; r_h is the hydrodynamic radius, η is the viscosity of water, k is the Boltzman constant. [b] Equation 2 in ref 47. [c] Core radius + head group radius (2 Å) + two layers of water (2 Å) associated with the charged micelles (SDS and CTAB). [d] Optimum value from light scattering experiments, ref 42. [e] Reference 49. [f] Reference 28.

The fluorescence anisotropy decay of the dye in a pure solvent (water or *n*-butanol) is single exponential. The values of r_0 and τ_r ($=\tau_{slow}$) are given in Table 1. In the case of micellar systems where the fluorescence decay is a single exponential, the fluorescence depolarization is solely due to the rotational dynamics of a single fluorophore species encapsulated in the micelle. The polarized fluorescence decays (parallel and

perpendicular components) were fitted to eqs 2 and 3. It was observed that a single-exponential function for $r(t)$ gave a poor fit to the data. However, a biexponential function for $r(t)$ (eq 6) was adequate to fit the data. The anisotropy decay has fast and slow components. The values of r_0, τ_{slow}, τ_{fast}, and β are given in Table 1. Figure 5 shows the parallel and perpendicular components of the fluorescence decay of nile red in the SDS micelle. The goodness of fit to $r(t)$ is shown in Figure 5B.

In the cases of CV in CTAB and TX or rhodamine B in all the micelles, the fluorescence originates from the dye distributed in aqueous and the micellar phases. The fluorescence decays at magic angle, parallel, and perpendicular polarization components are given by eqs 1, 8, and 9, respectively. $I_1(t)$ and $r_1(t)$ are the fluorescence and anisotropy decay functions in water, $I_2(t)$ and $r_2(t)$ are the corresponding functions in the micelle, and α is the fractional intensity in water. It was found that the polarized components of fluorescence decays were fitted poorly if $r_2(t)$ was assumed to be a single exponential. However, a biexponential equation for $r_2(t)$ (eq 6) was adequate to fit the data. The values for the anisotropy decay parameters of $r_2(t)$ for these cases are given in Table 1.

The fluorescence decay of DODCI in CTAB and TX is biexponential. However, Figure 3 shows that r_{ss} attains a constant value for $x > 2$, indicating that the dye is micellized for the experimental condition of $x = 30.4$ (CTAB) and $x = 38.5$ (TX). The two lifetimes are therefore associated with the dye in the micelle. In this case the parallel and perpendicular components of fluorescence were fitted to eqs 2 and 3, where $I(t)$ is biexponential. In these cases also, a biexponential function for $r(t)$ gave a good fit to the experimental data. The values of the anisotropy parameters are given in Table 1.

The effect of varying the temperature on the fluorescence intensity and anisotropy of nile red in SDS was studied in the temperature range 15−50 °C. Table 3 summarizes the variation of all the fluorescence and anisotropy parameters with temperature. Increasing temperature decreases the fluorescence lifetime, the steady-state anisotropy, and the anisotropy decay parameters, τ_{slow}, τ_{fast}, and β. r_0 is the only parameter that remains nearly constant with temperature.

Discussion

The structures of the micelles formed by the three surfactants used in this study have been well characterized. In dilute aqueous solutions, but above cmc, the surfactant molecules aggregate to form spherical micelles.[16,17,28] The fluorescence anisotropy decay of the dye molecule bound to the micelle is a consequence of the reorientation dynamics of the excited state of the molecule as well as that of the micelle. Several models for the reorientation dynamics of a molecule in the micelle are possible. There are at least two models (models 1 and 2 in Figure 6) that predict the anisotropy decay to be single exponential. In the first model (model 1) the dye molecule is rigidly attached to the micelle, and the reorientation dynamics for the molecule is identical with that of the spherical micelle which is single exponential with τ_M as the decay constant. In the second model (model 2) the dye molecule is in the core of the micelle (which may be considered as a homogeneous medium having physical properties resembling that of an oil drop), and the reorientation dynamics is single exponential with a time constant $(\tau_M^{-1} + \tau_r^{-1})^{-1}$, where τ_r is the anisotropy decay constant in the "oil drop". None of the anisotropy decays for the five dyes in the three micelles are single exponential, and hence the above two models are ruled out.

Models of reorientation dynamics predicting bi- and triexponential anisotropy decays have been considered before. For example, Klein and Haar[22] considered a model where the micelle-bound rhodamine 6G is fully exposed to the aqueous phase and the rotation of the fluorophore about a molecular axis was sufficient to account for the anisotropy decay. Chou and Wirth[38] also considered a similar model for acridine orange bound to the micelle. Visser et al.[25] have considered the model where the local dynamics of the dye is approximated to the wobbling-in-cone model for the dye solubilized in the interfacial region of the micelle. All the above models take into account the rotation of the micelle, but the possibility of reorientation of the dye as a result of the translational diffusion of the molecule in the micelle was not considered. In homogeneous media and in planar membranes, the translational diffusion of the molecule does not reorient the molecule. In a spherical micelle, the dye molecule is preferentially situated near the interface[19−21] and the molecule is oriented with respect to the interface (nonzero order parameter). For such a case translational diffusion on the two-dimensional spherical surface of the micelle is possible. The transport of the molecule along the spherical surface inevitably reorients the molecule with respect to its initial orientation. The fluorescence anisotropy decay function due to the surface transport depends upon the orientation of the molecule-fixed emission dipole with respect to the normal to the spherical surface. In the simplest case where the molecular dipole is parallel to the surface normal the reorientation dynamics due to transport of the molecule on the spherical surface is identical with the isotropic rotational diffusion of the molecule which is situated at the center of the sphere, and the following equality holds: $D_r = D_t/r_M^2$, where D_r is the isotropic rotational diffusion constant, D_t is the translational diffusion coefficient, and r_M is the radius of the micelle. For the case of isotropic rotational diffusion of a spherical rotor the correlation decay is single exponential and the time constant is $\tau_r = [l(l+1)D_r]^{-1}$.[51] For fluorescence depolarization experiments $l = 2$ and $\tau_r = (6D_r)^{-1}$. Thus, for the fluorescence depolarization due to surface transport the time constant is $\tau_D = r_M^2/6D_t$. Quitevis et al.[26] have included the translational diffusion of the dye together with the wobbling-in-cone dynamics model for the analysis of fluorescence anisotropy decays. (It may be noted however that the equation $\tau_D = r_M^2/4D_t$ given in ref 26 is incorrect.) In this model (model 4 in Figure 6), the contribution to the anisotropy decay comes from three independent motions: wobbling of the dye molecule in a restricted region (assumed for simplicity as a cone),[39,40] translational diffusion of the dye along the spherical surface, and rotation of the micelle as a whole. For this model $r(t)$ is given by eq 13:

$$r(t) = r_0[S^2 + (1 - S^2)\exp(-t/\tau_r)]\exp\{-t(1/\tau_D + 1/\tau_M)\} \quad (13)$$

r_0 is the initial anisotropy at $t = 0$, S^2 is the square of order parameter (which is a measure of the equilibrium orientational distribution of the dye[40]) for the intercalation of dye in the micelle, τ_r is the time constant for the wobbling motion of the dye, τ_D is the reorientation time constant due to the translational diffusion of the dye along the spherical micellar surface, and τ_M is the reorientation time constant for the spherical micelle. Comparison of eq 13 with biexponential eq 6, which was used to fit the experimental data, gives the following relations between the experimental and model parameters.

$$\beta = S^2 \quad (14)$$

$$1/\tau_{slow} = 1/\tau_D + 1/\tau_M \quad (15)$$

$$1/\tau_{fast} = 1/\tau_R + 1/\tau_D + 1/\tau_M \quad (16)$$

TABLE 3: Temperature Depencence of Rotational Dynamic Parameters

	nile red in SDS micelle											
T (°C)	τ_f (ns)	r_0	τ_{slow} (ns)	τ_{fast} (ns)	β	r_{ss}	τ_M (ns)	S	θ_0 (deg)	τ_d (ns)	$D_w \times 10^{-8}$ (s^{-1})	$D_t \times 10^{10}$ ($m^2\ s^{-1}$)
15	2.57	0.33	2.38	0.75	0.438	0.103	11.00	0.66	41.0	3.03	1.15	1.53
25	2.43	0.33	1.99	0.57	0.357	0.090	8.30	0.60	45.4	2.62	1.87	1.77
30	2.33	0.35	1.75	0.47	0.295	0.083	7.39	0.54	49.0	2.29	3.42	2.03
40	2.12	0.33	1.35	0.40	0.192	0.070	5.86	0.44	55.9	1.74	3.49	2.67
50	1.92	0.33	1.18	0.29	0.182	0.060	4.75	0.43	56.7	1.57	5.14	2.96

It is worth noting here that model 3 (Figure 6), which does not include lateral diffusion ($D_t = 0$ or $\tau_D = \infty$), predicts the anisotropy decay to be biexponential, which is also consistent with the experimental observation. However, model 3 predicts that the slow component, τ_{slow} must be equal to the rotational correlation time of the micelle, τ_M. Comparison of the experimental values of τ_{slow} (Table 1) for the five dyes in the three micelles with the value of τ_M (Table 2) shows that $\tau_{slow} \ll \tau_M$, and therefore model 3 is not applicable. Hence, lateral diffusion is an important mechanism of fluorescence depolarization.

The translational diffusion coefficient (D_t) is related to τ_D by eq 17.

$$D_t = r_M^2/6\tau_D \tag{17}$$

r_M is the radius of the spherical surface in which the dye diffuses. The wobbling rotational diffusion coefficient (D_w) is calculated using the anisotropy parameters τ_r and S. According to the wobbling-in-cone model,[40]

$$D_w = \{\tau_R(1 - S^2)\}^{-1}[-x^2(1 + x)^2\{1n[(1 + x)/2] + (1 - x)/2\}\{2(1 - x)\}^{-1} + (1 - x)(6 + 8x - x^2 - 12x^3 - 7x^4)/24] \tag{18}$$

where $x = \cos\theta_0$. θ_0 is the semicone angle in the wobbling-in-cone model, which is determined from the value of the order parameter and eq 19.[40]

$$S = 0.5\cos\theta_0(1 + \cos\theta_0) \tag{19}$$

From the above discussion and equations, it is clear that the micellar parameters τ_M and r_M must be known in order to calculate the structural (S and θ_0) and dynamical parameters (D_t and D_w) for the dye bound to the micelle. In this study, we have chosen the most extensively studied micellar systems whose structural and physical properties are well-known from the previous studies.[16,17,28] r_M is taken to be the core radius of the micelle. The lipid-labeled rhodamine DPPE was chosen in this study with an expectation that lateral diffusion would be negligible and thereby determine τ_M experimentally. However, even for this molecule lateral diffusion was appreciable and τ_{slow} was far less than the value of τ_M for the three micelles. The most important consideration for τ_M is the shape of the micelle, which is approximately spherical for all the cases (Table 2). For a spherical particle (micelle) τ_M is related to the volume, viscosity (η), and temperature by Stokes−Einstein relation (eq 20):

$$\tau_M = \frac{\eta 4\pi r_h^3}{3kT} \tag{20}$$

r_h is the hydrodynamic radius of the micelle. The calculated values for τ_M are given in Table 2 together with the radii and other data for the micelles.

TABLE 4: Values of the Parameters for the Model (Wobbling-in-Cone + Translational Diffusion) Derived from the Experimental Results (Dyes in Micelles)

dye/solvent/micelle	S	θ_0 (deg)	$D_w \times 10^{-8}$ (s^{-1})	$D_t \times 10^{10}$ ($m^2\ s^{-1}$)
nile red				
butanol	0.00	90	3.88	
SDS	0.60	45.4	1.86	1.77
CTAB	0.71	37.5	1.36	1.95
TX-100	0.79	31.5	0.34	3.31
cresyl violet				
butanol	0.00	90	2.22	
SDS	0.59	45.6	2.71	1.71
CTAB	0.67	40.2	0.92	1.47
TX-100	0.79	31.0	0.81	5.00
DODCI				
butanol	0.00	90	4.11	
SDS	0.76	34.1	1.21	1.75
CTAB	0.77	33.2	1.02	1.47
TX-100	0.88	23.4	0.73	5.00
rhodamine B				
butanol	0.00	90	3.08	
SDS	0.75	34.6	2.39	1.43
CTAB	0.55	48.6	1.03	1.35
TX-100	0.75	34.6	0.70	3.53
rhodamine-DPPE				
SDS	0.62	54.2	0.61	0.73
CTAB	0.84	27.2	0.63	0.53
TX-100	0.69	39.0	0.41	0.73

The values for S, τ_r, τ_D, D_t, D_w, and θ_0 were calculated for nile red, CV, DODCI, rhodamine B, and rhodamine-DPPE in SDS, CTAB, and TX micelles and are given in Table 4. The values for these dyes in water and butanol are also given for comparison. The value of D_w in butanol was obtained using $D_w = (6\tau_r)^{-1}$. The values of D_w in the micelle were calculated using eq 18.

Order Parameter and θ_0. The order parameter for the dye molecules in butanol is zero because the dye molecule tumbles freely and the equilibrium orientational distribution is completely random. The order parameter for all the dye probes in the micelles is in the range 0.55−0.88 (θ_0 varying from 45° to 27°), indicating that the equilibrium orientational distribution is highly constrained because of the aqueous/nonaqueous interface in the micelle. That is, the dye molecules do have a preferential orientation with respect to the interface. As will be discussed in a later section (temperature study) the order parameter decreases with increasing mobility (diffusion) of the dye in the micelle.

Wobbling Diffusion Coefficient. According to the wobbling-in-cone model, the molecule wobbles freely inside a cone of semiangle θ_0. The values for θ_0 and wobbling diffusion coefficient, D_w, are the quantitative parameters for this model. The results shown in Table 4 indicate that the wobbling diffusion coefficients of all the dye molecules, excluding rhodamine DPPE, are in the range $(0.34-2.7) \times 10^8\ s^{-1}$. These values are a factor 2−6 less than the rotational diffusion coefficient for the same dye in *n*-butanol, where the wobbling is free. The rotational diffusion coefficient is the least for the rhodamine-DPPE even though the cone angle is not very different from

that of other dyes. The slow wobbling (and similarly slow translational diffusion) for rhodamine-DPPE indicates that covalent linking with the lipid chain does affect the diffusive dynamics of the dye molecule. The comparison of the diffusion coefficients for the same dye in different micelles indicates a consistent observation that the wobbling diffusion coefficient is less in TX than in SDS and CTAB for the same dye irrespective of their structural differences. Similar observations of lower wobbling diffusion coefficient in the TX micelle have also been observed for other fluorescent molecules: porphyrins[31] and merocyanine 540 and octadecylrhodamine B.[26] A similar but opposite trend is observed for D_t (see below).

Translational (Lateral) Diffusion Coefficient. The translational diffusion coefficient of the dye molecule on the micellar surface is lowest for rhodamine-DPPE, which is to be expected. For other dye molecules the value is in the range $(1.4-5.0) \times 10^{-6}$ cm^2 s^{-1}. These values are comparable to or larger than the lateral self-diffusion coefficient ($(0.2-1.5) \times 10^{-6}$ cm^2 s^{-1}) of surfactant molecules in SDS or CTAB micelle.[41,42] One interesting observation is the consistently larger diffusion coefficient for all dyes (except rhodamine-DPPE) in TX than in SDS or CTAB. This is exactly opposite of that observed for the wobbling diffusion coefficient and is discussed further in a later section.

Temperature Effects on D_w, D_t, S, and θ_0. The micellar structure is compact but fluidlike, as indicated by the wobbling and lateral diffusion of the dye molecules. The variation of the structural and dynamical fluidity parameters of nile red in SDS micelle was investigated at different temperatures (15−50 °C). The fluorescence decay of nile red in SDS micelle at magic angle polarization was fitted adequately (χ^2 varying from 0.9 to 1.1) to a single-exponential function at all temperatures. This indicated that the partitioning of nile red in aqueous phase was negligible even at 50 °C, which is not surprising since the dye is neutral and insoluble in water. It was observed however that the fluorescence lifetime of the dye in the micelle decreased with increasing temperature. Such a decrease of lifetime with temperature is usually associated with an increase in nonradiative rate with temperature. Nile red has a diethyl amino group which can undergo torsional motion about the C−N bond, which can increase the nonradiative rate. Interestingly, the temperature dependence of the lifetime of nile red in butanol was only marginal (3.90 ns at 25 °C and 3.72 ns at 50 °C) compared to the temperature dependence in the micelle (2.43 ns at 25 °C and 1.92 ns at 50 °C). This is an indication that the temperature dependence of the torsional motion of nile red in the micelle is quantitatively different than in butanol; that is, the torsional motion appears to be faster in the micelle, which is in qualitative agreement with a similar strong temperature dependence of D_w (see below). The experimentally determined fluorescence anisotropy parameters for nile red in SDS at different temperatures (Table 3) were used to calculate D_w, D_t, S, and θ_0. It is assumed that the aggregation number and radius of the micelle remain unchanged in this temperature range.[50] Table 3 shows the variation of D_w, D_t, S, and θ_0 with temperature. It is observed that D_w and D_t increase with temperature. However, the value of D_w increases by a factor of 4.5, whereas D_t increases by only 1.9 in the above temperature range. The order parameter decreases with temperature, and the cone semiangle calculated from the order parameter increases from 41° to 56.7° in the temperature range 15−50 °C. Increased mobility of the dye molecule seems to have the effect of increasing the cone angle. These results indicate that an increase in diffusion coefficient is correlated with a decrease in order parameter.

Microviscosity. In the classical model of the micelle the interior region of the micelle is considered to be liquidlike and the physical properties of the interior would resemble that of an oil drop. The fact that all organic substances that are insoluble in water could be solubilized in aqueous micellar solutions had a facile explanation that organic molecules seek the interior hydrocarbon region of the micelle. This led to the assumption that the physical properties of the "oil drop" (viscosity, dielectric constant, etc.) could be determined using the solubilized organic molecule as the probe. Shinitzky et al.[43] used the steady-state fluorescence anisotropy (which is larger in micellar solutions than in water or alcohol) of several organic molecules and calculated the "microviscosity" of the interior region of the micelle. The crucial assumptions involved are (a) the organic molecule is solubilized in the interior region, (b) the molecule tumbles freely in the micelle as in a pure solvent, and (c) the Stokes−Einstein equation for the rotational diffusion coefficient and correlation time ($D_r = kT/8\pi\eta r^3$ and $\tau_r = (6D_r)^{-1}$) for a spherical particle in liquid is valid for the micellar interior. The microviscosity for several micelles (including SDS and CTAB) was in the range 15−50 cP at room temperature, and the value for the same micelle depends on the probe.[43] The microviscosity of the micelle was also determined using other spectroscopic properties of the solubilized molecules and their relationship to lateral or rotational diffusion coefficient of the molecule. To give a few examples, ESR of organic free radicals trapped in micelles was used to determine the diffusion coefficient in the micelle,[44] which gives the microviscosity for SDS to be approximately 5 cP.[44] Intermolecular excimer formation kinetic data of pyrene in micelles were used, and the microviscosities of SDS and CTAB were determined to be 193 and 151 cP, respectively,[45] whereas intramolecular excimer formation kinetics led to a value of 4 cP.[46] The discrepancy in the results was substantially large, and the value of "microviscosity" is technique-dependent and also probe-dependent. It is evident that one or more of the basic assumptions stated above concerning the diffusive dynamics of the solubilized molecule in micelles is not valid.

The sites of solubilization of organic molecules in micelles (usually SDS or CTAB) have been investigated extensively.[19−21] It appears that practically all organic molecules are solubilized near the surface, even for small aromatic molecules such as benzene.[20] Therefore, organic molecular probes are expected to report the physical properties of the interfacial region and not that of the interior region. Since the interfacial region is structurally heterogeneous (consisting of polar and nonpolar regions separated by a few angstroms), the structure and dynamics of organic probe molecules would be sensitive to the nature of the probe molecule. For example, the dynamics of a charged probe molecule would be different from that of a neutral probe molecule. Moreover, the equilibrium orientational distribution of the probe molecule in the site of solubilization in micelles is not random (nonzero order parameters), and hence the assumption of free tumbling of the probe molecule in micelles is also incorrect. These factors could explain the sensitivity of the microviscosity value to the nature of the probe and the technique used. Thus, it is important that a proper modeling of the diffusive dynamics of the probe and an appropriate experimental technique, preferably the time-resolved technique, are necessary. The question remains whether "microviscosity" itself is meaningful or not for the micelle.

The techniaue of time-resolved fluorescence used in this study gives a direct measurement of the diffusive dynamics of the fluorescence molecule in the micelle. The analysis of the fluorescence data for five organic dyes ruled out some simple models (models 1 and 2 in Figure 6) for the dynamics of the molecule. The most appropriate model of dynamics consisted

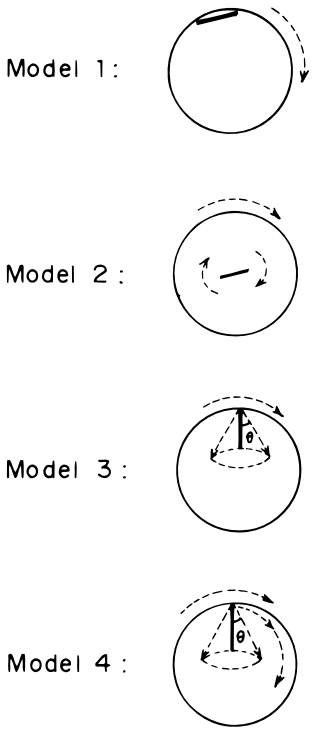

Figure 6. Different models of the fluorescence dynamics in micelles.

of wobbling of the molecular in a restricted space (wobbling-in-cone), lateral diffusion along the spherical surface, and rotation of the micelle. This model is also consistent with the observation that the dyes are solubilized near the surface. The analysis of data led to the determination of D_w and D_t for the probe molecule. These values can be used to test the usefulness of the concept of "microviscosity" in micelles.

D_w and D_t and the ratio (D_t/D_w) are related to microviscosity by Stokes−Einstein eqs 21 and 22.

$$D_w = \frac{\zeta kT}{6\eta V} \tag{21}$$

$$D_t = \frac{\zeta' kT}{6\pi\eta r} \tag{22}$$

$$\frac{D_t}{D_w} = \frac{\zeta'}{\zeta}\frac{4r^2}{3} \tag{23}$$

Here ζ and ζ' are constants that are correction factors for the nonspherical shape of the molecule,[48] r is the radius, and V is the molecular volume of the probe. One expects the ratio D_t/D_w to be independent of temperature for the same probe. Figure 7 shows the plot of D_t/D_w as a function of temperature for the neutral dye probe, nile red, in SDS micelles (data from Table 3). The ratio decreases with increasing temperature even in the small temperature range 288−323 K. Therefore, the Stokes−Einstein equations for D_t and D_w are not valid for the probe solubilized in the micelle. Failure of the Stokes−Einstein equation is an indication of "non-Brownian" dynamics, and we conclude that the "microviscosity" is an ill-defined parameter in such a system.

There are two possible reasons for the failure of the Stokes−Einstein relations to describe correctly the diffusive dynamics of the molecular probe in micelles. First, the Brownian dynamics of collisions between solute (probe) and solvent (surfactant molecule) in micelles and the transfer of linear and angular momenta are fundamentally different (for example, a hopping mechanism for lateral diffusion; see below) from that

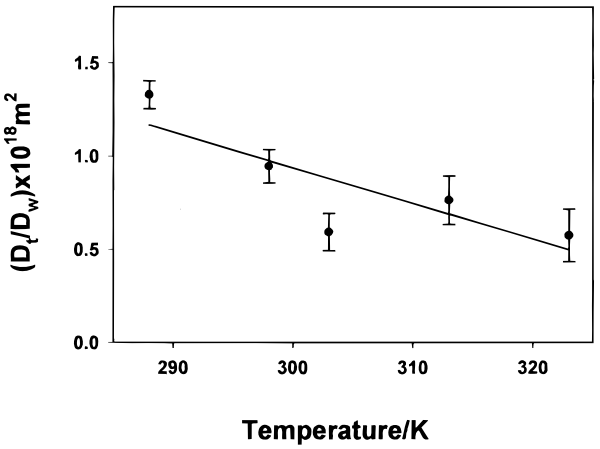

Figure 7. Plot of D_t/D_w vs temperature for nile red in SDS micelles.

in liquids because of the nonrandom orientational distribution of the solute in micelles. Second, the length scale of the micelle, especially the interfacial region, is of the same order or possibly smaller than the probe molecule. Therefore, the concept of microviscosity in micelles can be convincingly tested only with a fluorescent probe that is solubilized in the core of the micelle (model 2 in Figure 6), where the fluorescence anisotropy decay is single exponential and the order parameter is zero. It will be interesting if such a fluorophore−micelle system could be identified.

Finally, we comment on the observation of faster lateral diffusion and slower wobbling diffusion of all the dye molecules (neutral and charged), including those reported for other molecules,[26,31] in neutral TX-100 than in negatively charged SDS or positively charged CTAB. TX-100 is larger in size and the surface is uncharged. It is conceivable that the basic mechanism of lateral diffusion of the solute is different in TX-100. For example, transport of the solute on the surface by a hopping mechanism is possible. Such a hopping is essentially a large amplitude motion of the solute which is confined to a small diffusive volume characteristic of a high-order parameter. Independent experiments and molecular dynamics simulations are necessary to assess the importance of hopping of solutes in micelles.

Conclusions

Fluorescence depolarization dynamics of a few organic dye molecules in three micelles is best described by a model of rotational (wobbling-in-cone) and translational diffusion of the dye coupled with the rotation of the micelle as a whole. The rotational and translational diffusion coefficients, order parameter, and semicone angle were determined. The order parameter is inversely correlated with the diffusion coefficient, which is expected. The rotational and translational diffusion coefficients do not follow the trend predicted by Stokes−Einstein equations, indicating the non-Brownian dynamics of the dye in the micelle.

References and Notes

(1) Fleming, G. R. In *Chemical Applications of Ultrafast Spectroscopy*; Oxford University Press: New York, 1986.
(2) Fleming, G. R.; Knight, A. E. W.; Morris, J. M.; Robbins, R. J.; Robinson, G. W. *Chem. Phys. Lett.* **1977**, *51*, 399.
(3) Sadkowski, P. J.; Fleming, G. R. *Chem. Phys. Lett.* **1978**, *57*, 526.
(4) Cramer, L. E.; Spears, K. G. *J. Am. Chem. Soc.* **1978**, *100*, 221.
(5) Beddard G.; Doust, T.; Porter, G. *Chem. Phys.* **1981**, *61*, 17.
(6) von Jena, A.; Lessing, H. E. *Chem. Phys. Lett.* **1981**, *78*, 187.
(7) Dutt, G. B.; Doraiswamy, S.; Periasamy, N.; Venkataraman, B. *J. Chem. Phys.* **1990**, *93*, 8498.
(8) Dutt, G. B.; Doraiswamy, S.; Periasamy, N. *J. Chem. Phys.* **1991**, *94*, 5360.

(9) Roy, M.; Doraiswamy, S. *J. Chem. Phys.* **1993**, *98*, 3213.
(10) Hartman, R. S.; Alavi, D. S.; Waldeck, D. H. *J. Phys. Chem.* **1991**, *95*, 7872.
(11) Hartman, R. S.; Waldeck, D. H. *J. Phys. Chem.* **1994**, *98*, 1386.
(12) Weber, G. *J. Chem. Phys.* **1977**, *66*, 4801.
(13) Mantulin, W. W.; Weber, G. *J. Chem. Phys.* **1977**, *66*, 4092.
(14) Christensen, R. L.; Drake, R. C.; Phillips, D. *J. Phys. Chem.* **1986**, *90*, 5960.
(15) Kim, Y. R.; Hochstrasser, R. M. *J. Phys. Chem.* **1992**, *96*, 9595.
(16) Mittal, K. L., Ed. *Micellisation, Solubilisation and Microemulsions*; Plenum: New York, 1977; Vols. 1 and 2.
(17) Fendler, J. H. *Membrane Mimetic Chemistry*; Wiley-Interscience: New York, 1982.
(18) Lindman, B.; Wennerstrom, H. *Top. Curr. Chem.* **1980**, 1.
(19) Mukerjee, P. *Solution Chemistry of Surfactants*; Mittal, K. L., Ed.; Plenum Press: New York, 1979; Vol. 1.
(20) Mukerjee, P.; Cardinal, J. R. *J. Phys. Chem.* **1978**, *82*, 1620.
(21) Ganesh, K. N.; Mitra, P.; Balasubramanian, D. *J. Phys. Chem.* **1982**, *86*, 4291.
(22) Klein, U. K. A.; Haar, H.-P. *Chem. Phys. Lett.* **1978**, *58*, 531.
(23) Lessing, H. E.; von Jena, A. *Chem. Phys.* **1979**, *41*, 395.
(24) Reed, W.; Politi, M. J.; Fendler, J. H. *J. Am. Chem. Soc.* **1981**, *103*, 4591.
(25) Visser, A. J. W. G.; Vos, K.; van Hoek, A.; Santema, J. S. *J. Phys. Chem.* **1988**, *92*, 759.
(26) Quitevis, E. L.; Marcus, A. H.; Fayer, M. D. *J. Phys. Chem.* **1993**, *97*, 5762.
(27) Turro, N. J.; Gratzel, M.; Braun, A. M. *Angew. Chem.* **1980**, *19*, 670.
(28) Kalyanasundaram, K. *Photochemistry in Microheterogeneous Systems*; Academic Press: New York, 1991.
(29) Periasamy, N.; Doraiswamy, S.; Maiya, G. B.; Venkataraman, B. *J. Chem. Phys.* **1988**, *88*, 1638.
(30) Bankar, K. V.; Bhagat, V. R.; Ranjan Das; Doraiswamy, S.; Ghangrekar, A. S.; Kamat, D. S.; Periasamy, N.; Srivatsavoy, V. J. P.; Venkataraman, B. *Indian J. Pure Appl. Phys.* **1989**, *27*, 416.
(31) Maiti, N. C.; Mazumdar, S.; Periasamy, N. *J. Phys. Chem.* **1995**, *99*, 10708.
(32) O'Connor, D. V.; Phillips, D. *Time-correlated Single Photon Counting*; Academic: London, 1984.
(33) Bevington, P. R. *Data Reduction and Error Analysis for the Physical Sciences*; McGraw-Hill: New York, 1969.
(34) Press, W. H.; Teukolsky, S. A.; Vettering, W. T.; Flannery, B. P. *Numerical Recipes in C. The Art of Scientific Computing*; Cambridge University Press: Cambridge, 1992.
(35) Cross, A. J.; Fleming, G. R. *Biophys. J.* **1984**, *46*, 45.
(36) Knutson, J. R.; Beechem, J. M.; Brand, L. *Chem. Phys. Lett.* **1983**, *102*, 501.
(37) Demas, J. N. *Excited-State Lifetime Measurements*; Academic Press: New York, 1983.
(38) Chou, S. H.; Wirth, M. J. *J. Phys. Chem.* **1989**, *93*, 7694.
(39) Kinosita, K. S.; Kawato, S.; Ikegami, A. *Biophys. J.* **1977**, *20*, 289.
(40) Lipari, G.; Szabo, A. *Biophys. J.* **1980**, *30*, 489.
(41) Ahlnas, T.; Soderman, O.; Hjelm, C.; Lindman, B. *J. Phys. Chem.* **1983**, *87*, 822.
(42) Nery, H.; Soderman, O.; Canet, D.; Walderhaug, H.; Lindman, B. *J. Phys. Chem.* **1986**, *90*, 5802.
(43) Shinitzkey, M.; Dianox, A. C.; Gitter, C.; Webber, G. *Biochemistry* **1971**, *10*, 2106.
(44) Waggoner, A. S.; Griffith, O. H.; Christensen, C. R. *Proc. Natl. Acad. Sci. U.S.A.* **1967**, *57*, 1198.
(45) Pownall, H. J.; Smith, L. C. *J. Am. Chem. Soc.* **1973**, *95*, 3136.
(46) Zachariasse, K. *Chem. Phys. Lett.* **1978**, *57*, 429.
(47) Tanford, C. *J. Phys. Chem.* **1972**, *76*, 3020.
(48) Edward, J. T. *J. Chem. Educ.* **1970**, *47*, 261.
(49) Robson, R. J.; Dennis, E. A. *J. Phys. Chem.* **1977**, *81*, 1075.
(50) Mazer, N. A; Benedek, G. B.; Casey, M. C. *J. Phys. Chem.* **1976**, *80*, 1075.
(51) Abragam, A. *The Principles of Nuclear Magnetism*; Clarendon Press: Oxford, 1961; pp 298−299.